Brain Cell Biology Volume 36, 141–154, 2008
DOI: 10.1007/s11068-008-9034-7

Improved expression of halorhodopsin for light-induced silencing of neuronal activity

Shengli Zhao[1], Catarina Cunha[1,2], Feng Zhang[3], Qun Liu[4], Bernd Gloss[4], Karl Deisseroth[3], George J. Augustine[1] and Guoping Feng[1,4,*]
[1]Department of Neurobiology, Duke University Medical Center, Box 3209, Research Drive, Durham, NC 27710, USA (*author for correspondence; e-mail: feng@neuro.duke.edu)
[2]Faculdade de Ciências da Universidade do Porto, Porto, Portugal
[3]Department of Bioengineering, Stanford University, Stanford, CA 94305, USA
[4]Duke Neurotransgenic Laboratory, Duke University Medical Center, Box 3209, Durham, NC 27710, USA

Received 8 June 2008; Revised 30 August 2008; Accepted 3 September 2008
Published online 17 October 2008

The ability to control and manipulate neuronal activity within an intact mammalian brain is of key importance for mapping functional connectivity and for dissecting the neural circuitry underlying behaviors. We have previously generated transgenic mice that express channelrhodopsin-2 for light-induced activation of neurons and mapping of neural circuits. Here we describe transgenic mice that express halorhodopsin (NpHR), a light-driven chloride pump that can be used to silence neuronal activity via light. Using the Thy-1 promoter to target NpHR expression to neurons, we found that neurons in these mice expressed high levels of NpHR-YFP and that illumination of cortical pyramidal neurons expressing NpHR-YFP led to rapid, reversible photoinhibition of action potential firing in these cells. However, NpHR-YFP expression led to the formation of numerous intracellular blebs, which may disrupt neuronal function. Labeling of various subcellular markers indicated that the blebs arise from retention of NpHR-YFP in the endoplasmic reticulum. By improving the signal peptide sequence and adding an ER export signal to NpHR-YFP, we eliminated the formation of blebs and dramatically increased the membrane expression of NpHR-YFP. Thus, the improved version of NpHR should serve as an excellent tool for neuronal silencing *in vitro* and *in vivo*.

Introduction

The complex and diverse functions of the brain depend on the unique properties of neural circuits formed by various subtypes of neurons with distinct molecular and electrical properties. Furthermore, many neurological disorders are often due to the dysfunction of specific subsets of neurons or neural circuits. Thus, elucidating the unique roles of each subtype of neuron in shaping circuitry function is critical to our understanding of both normal and abnormal brain function. This effort has been greatly facilitated by the recent development of optogenetic approaches for high-speed, light-induced activation or silencing of neurons through the use of light-sensitive, cation permeable channelrhodopsin-2 (ChR2), and the light-driven chloride pump halorhodopsin (NpHR) (Lanyi, 1990; Nagel et al., 2003; Boyden et al., 2005; Li et al., 2005; Bi et al., 2006; Zhang et al., 2006, 2007a, b, 2008; Han and Boyden, 2007; Petreanu et al., 2007; Zhang and Oertner, 2007; Gradinaru et al., 2007; Ernst et al., 2008). We have previously

generated transgenic mice that express ChR2 in subsets of neurons and demonstrated their utility for *in vivo* light-induced activation and mapping of neural circuits (Arenkiel et al., 2007; Wang et al., 2007). Consequently, genetic tools that permit photoinhibition of neuronal activity in mice using NpHR would complement the currently available ChR2 transgenic mice (JAX stock number 007615 and 007612), and significantly enhance our capability to dissect the cellular basis of circuitry function and dysfunction.

NpHR is a halorhodopsin isolated from the halophilic bacterium *Natronobacterium pharaonis* (Lanyi, 1990). It is a seven-transmembrane protein and functions as a light-driven chloride pump (Lanyi et al., 1990; Kolbe et al., 2000). Recent studies have demonstrated that expression of NpHR in mammalian neurons by transfection or viral infection allows rapid, light-induced reversible inhibition of neuronal activity (Zhang et al., 2007a; Han and Boyden, 2007; Gradinaru et al., 2007). Furthermore, transgenic expression of NpHR in *C. elegans* permits rapid control of motor behavior by light, illustrating the potential in using NpHR as a genetic tool to determine cellular and circuitry bases of behavior (Zhang et al., 2007a). To expand this tool into a mammalian model system, we generated transgenic mice that express NpHR-YFP using the neuron-specific Thy1 promoter. We found that high levels of NpHR-YFP were expressed in subsets of neurons in these mice and that illumination of NpHR-expressing neurons led to rapid, reversible photoinhibition of action potential firing in these cells. However, we found that NpHR-YFP was not efficiently targeted to plasma membrane and that high levels of NpHR-YFP expression in transgenic mice led to the formation of numerous intracellular blebs in neurons. Similar blebs have also been found in transfected or viral infected neurons (Gradinaru et al., 2008). Using markers of various subcellular compartments we determined that the blebs arose due to retention of NpHR-YFP in the ER. To improve the expression of NpHR we introduced an improved signal peptide sequence and added an ER export signal to NpHR-YFP. The modified NpHR-YFP showed dramatically increased membrane expression and no bleb formation in transfected neurons. The improved version of NpHR-YFP should serve as an excellent tool for neuronal silencing *in vitro* and *in vivo*.

Results

Thy1-NpHR-YFP transgenic mice

We used the well-characterized mouse Thy1 promoter to drive codon-humanized NpHR-YFP expression specifically in neurons in transgenic mice. Our previous studies have shown that the modified Thy1 promoter predominantly drives transgene expression in subsets of projection neurons, and that due to transgenic position-effect variegation, transgene expression is often restricted to different subsets of neurons in different transgenic lines (Feng et al., 2000; Arenkiel et al., 2007; Wang et al., 2007). We generated 7 founder lines, 5 of which showed NpHR-YFP expression in the brain. Expression of NpHR in lines 1, 3 and 7 was widespread, including layer V pyramidal neurons of the cortex, CA1 and CA3 pyramidal neurons and dentate granule cells of the hippocampus, and various neurons in the superior and inferior colliculus, thalamus, and brain stem (Fig. 1a–c and data not shown). In lines 6 and 9, NpHR-YFP expression was detected in isolated single neurons throughout various regions of the brain (Fig. 1d, e).

All Thy1-NpHR-YFP mice are viable and breed normally. However, we noticed two problems at the cellular level. First, unlike ChR2-YFP, which is mostly targeted to the plasma membrane in neurons of Thy1-ChR2-YFP mice (Arenkiel et al., 2007; Wang et al., 2007), a large fraction of the NpHR appeared to be cytoplasmic (Fig. 2a, b). In Thy1-ChR2-YFP mice, the intensity of the YFP fluorescence signal was highest in neuronal compartments with a high surface/volume ratio, such as in dendrites and axons (Arenkiel et al., 2007; Wang et al., 2007), whereas in Thy1-NpHR-YFP mice, the highest YFP fluorescence signal was in cell body layers (Fig. 2a, b). These observations suggest that NpHR-YFP is not efficiently targeted to the plasma membrane. The second problem is that NpHR-YFP formed numerous bright intracellular blebs, evident as brightly fluorescent, spherical structures often found in neurons expressing NpHR (Fig. 2c, d). This was particularly apparent in transgenic lines that express high levels of NpHR-YFP, such as lines 3 and 7 (Fig. 2e, f). These blebs varied in size and could form in cell bodies or in dendrites (Fig. 2c, d). Large blebs often caused dramatic, local swelling of dendrites (Fig. 2d), raising the concern that these blebs could affect neuronal functional properties.

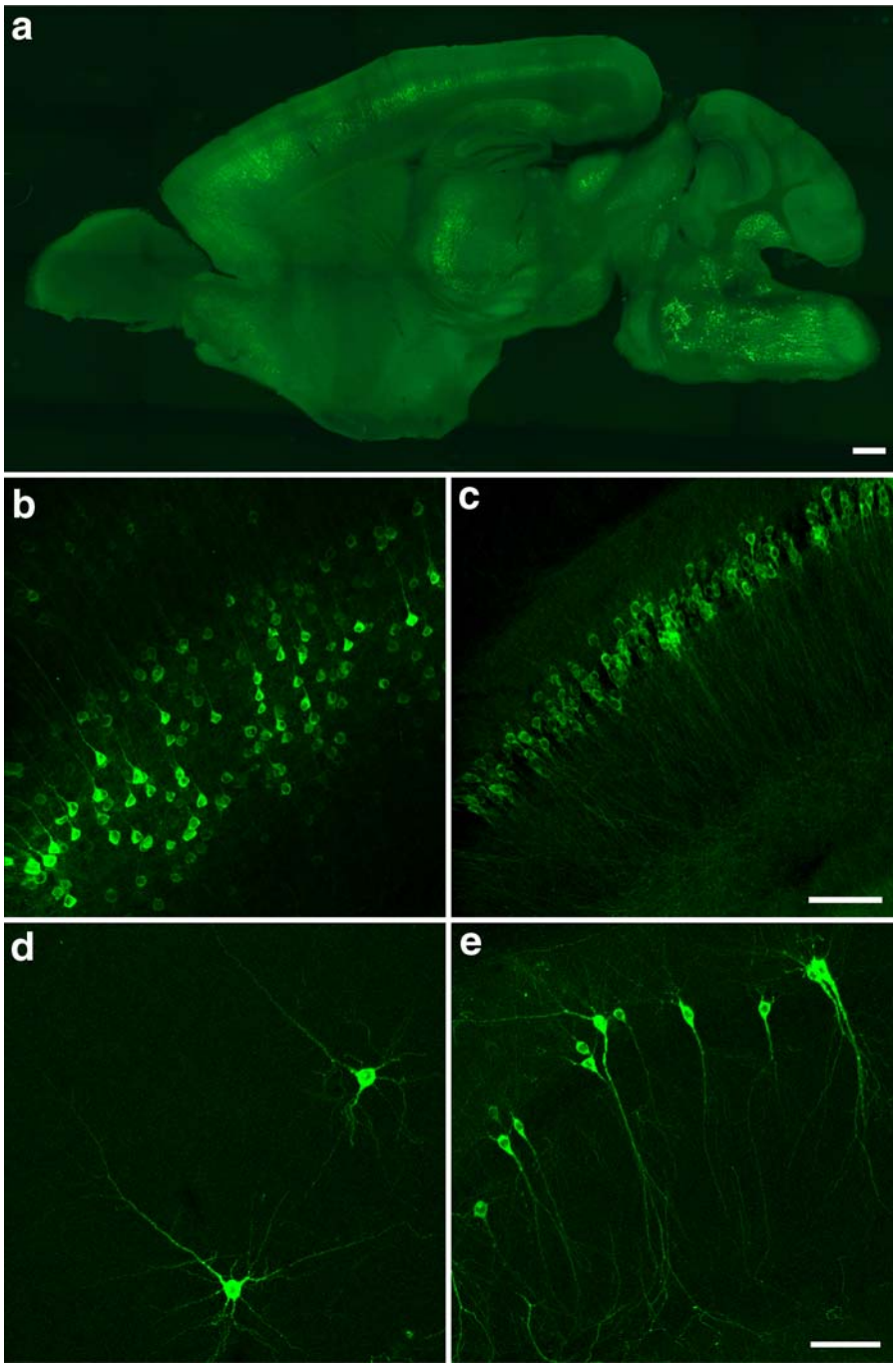

Fig. 1. Thy1-NpHR-YFP transgenic mice. (a) An image of a sagittal brain section from an adult Thy1-NpHR-YFP transgenic mouse (line 1). (b, c) Confocal images showing the expression of NpHR-YFP in layer V pyramidal neurons of the cortex (b) and CA1 pyramidal neurons of the hippocampus (c) in Thy1-NpHR-YFP mice (line 1). (d, e) Confocal images showing that NpHR is expressed sparsely in cortex and CA1 of the hippocampus in line 6 Thy1-NpHR-YFP transgenic mice. Scale bars, 500 μm in a, 100 μm in c for b and c, and 100 μm in e for d and e.

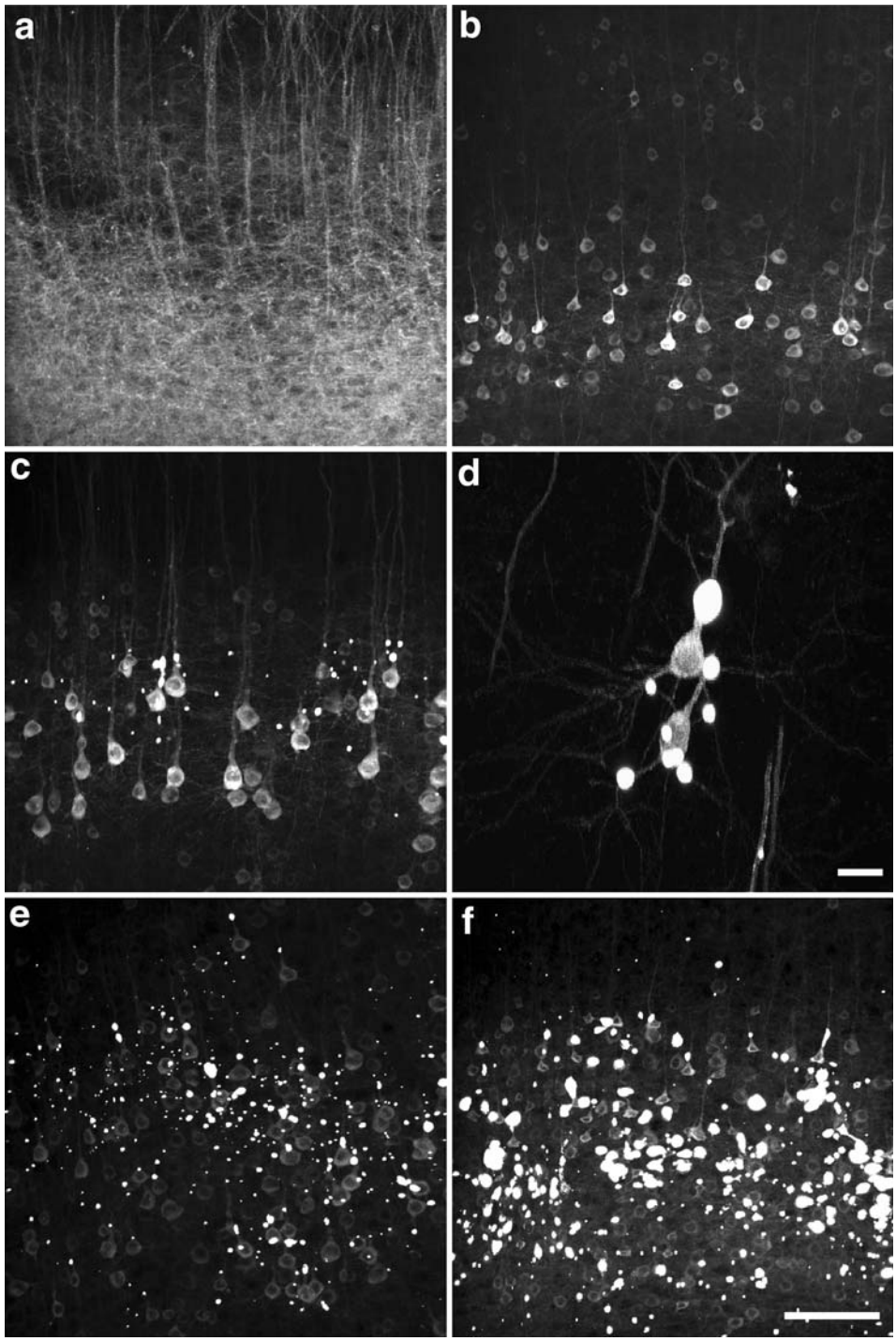

Fig. 2. Poor membrane expression and intracellular blebs in Thy1-NpHR-YFP mice. (a) In Thy1-ChR2-YFP transgenic mice, ChR2-YFP is efficiently targeted to the plasma membrane, as the intensity of YFP fluorescence signal is highest where the cells have a high surface/volume ratio as in dendrites. (b) In Thy1-NpHR-YFP transgenic mice, NpHR-YFP is mostly retained in cell bodies and proximal dendrites (line 1). (c–f) NpHR-YFP forms numerous intracellular blebs in neurons of Thy1-NpHR-YFP transgenic mice. Images are from the cortex of line 1 (c), 6 (d), 3 (e), and 7 (f) mice. Scale bars, 20 μm in d, 100 μm in f for a–c, and e, f.

Photoinhibition of NpHR-YFP expressing cells

To determine whether transgenic expression of NpHR-YFP in mice allows light-induced inhibition of neuronal activity, we characterized the electrophysiological properties of neurons in a line of Thy1-NpHR-YFP mice with minimal blebbing (line 6; Fig. 1d, e).

We first asked whether NpHR expression altered the functional characteristics of neurons. For this purpose, we used whole-cell patch clamp recordings to measure the electrophysiological properties of NpHR-expressing pyramidal neurons in slices from the hippocampus and cortex of line 6 mice. No significant differences were observed between the resting electrical properties of NpHR-positive and NpHR-negative neurons, or in the ability of these neurons to generate action potentials (Table 1). We, therefore, conclude that in the absence of illumination, NpHR expression does not affect the electrical properties of these neurons despite the presence of some blebbing.

We next asked whether illumination of NpHR could photoinhibit neurons. For this purpose, large light spots ($\approx$0.4 mm^2) of yellow light (545–585 nm; 1 s duration) were used to illuminate cortical and hippocampal slices. In both brain regions, illumination of NpHR-positive pyramidal neurons generated outward currents (Fig. 3a). No currents were evoked during illumination of NpHR-negative neurons (data not shown), demonstrating that the currents were due to activation of NpHR. At maximal excitation light intensity, the time constant for activation of these currents during the light pulse was 7.0 $\pm$ 0.5 ms and the time constant for deactivation of the currents following the end of illumination was 7.0 $\pm$ 0.5 ms.

The magnitude of the NpHR-mediated photocurrent depended upon light intensity, with stronger illumination yielding larger currents (Fig. 3a). This relationship arises from progressive activation of more NpHR pumps as the light intensity increases. The relationship between light intensity and peak amplitude of the photocurrent could be described by the Hill equation (Fig. 3b):

$$Y = I_{\max}\frac{X^n}{K^n + X^n}$$

where X is light luminance and K represents the light level where the photocurrent was half-maximal (15 $\pm$ 0.2 mW/mm^2). I_{max}, the maximum current amplitude, was 68 $\pm$ 5.5 pA and n, the Hill coefficient, was 1.1 $\pm$ 0.1. The Hill coefficient of approximately 1 indicates that absorption of a single photon is sufficient for activation of NpHR, even though NpHR is known to trimerize (Kolbe et al., 2000).

In current-clamp conditions, illumination (1 s long light flashes) of NpHR produced small hyperpolarizations of the membrane potential (Fig. 3c). At maximal excitation light intensity, the time required to reach the half-maximal change in membrane potential was 23 $\pm$ 4 ms and the half-time for repolarization of the membrane potential after illumination ended was 19.3 $\pm$ 3.2 ms. As was the case for NpHR-mediated currents, the magnitude of these hyperpolarizations depended upon light intensity. The relationship between the amplitude of these potential changes and light luminance again was a saturable function that could be described by the Hill equation (Fig. 3d). The derived values of K (13 $\pm$ 0.1 mW/mm^2) and Hill coefficient (0.8 $\pm$ 0.1) were similar to those determined for the light-induced photocurrents (1.1 $\pm$ 0.1), while the maximal voltage change was 8.9 $\pm$ 2.5 mV (n = 5).

To examine the effects of NpHR activation on neuronal excitability, NpHR-positive pyramidal neurons in the cortex and hippocampus were stimulated with depolarizing current pulses (2 s duration) to evoke trains of action potentials (Fig. 3e, top). Subsequent illumination reduced the AP frequency in a light-dependent manner (Fig. 3e, lower traces;

Table 1. Comparison of electrical properties of wildtype and NpHR expressing neurons

Genotype	Action potential amplitude (mV)	Action potential duration (ms)	Input resistance (MΩ)	Resting potential (mV)	Threshold (mV)
NpHR$^-$	55.1 $\pm$ 10.4	2.24 $\pm$ 0.4	147.2 $\pm$ 13.7	–62.5 $\pm$ 3.4	–32.5 $\pm$ 4.3
NpHR$^+$	48.3 $\pm$ 6.3	2.11 $\pm$ 0.3	148.7 $\pm$ 33.6	–62.0 $\pm$ 3.5	–29.3 $\pm$ 3.7

Sample size is 10 cells for each group. There was no statistical significant difference ($P > 0.05$; t-test) in the mean value of any parameter between the two types of neurons.

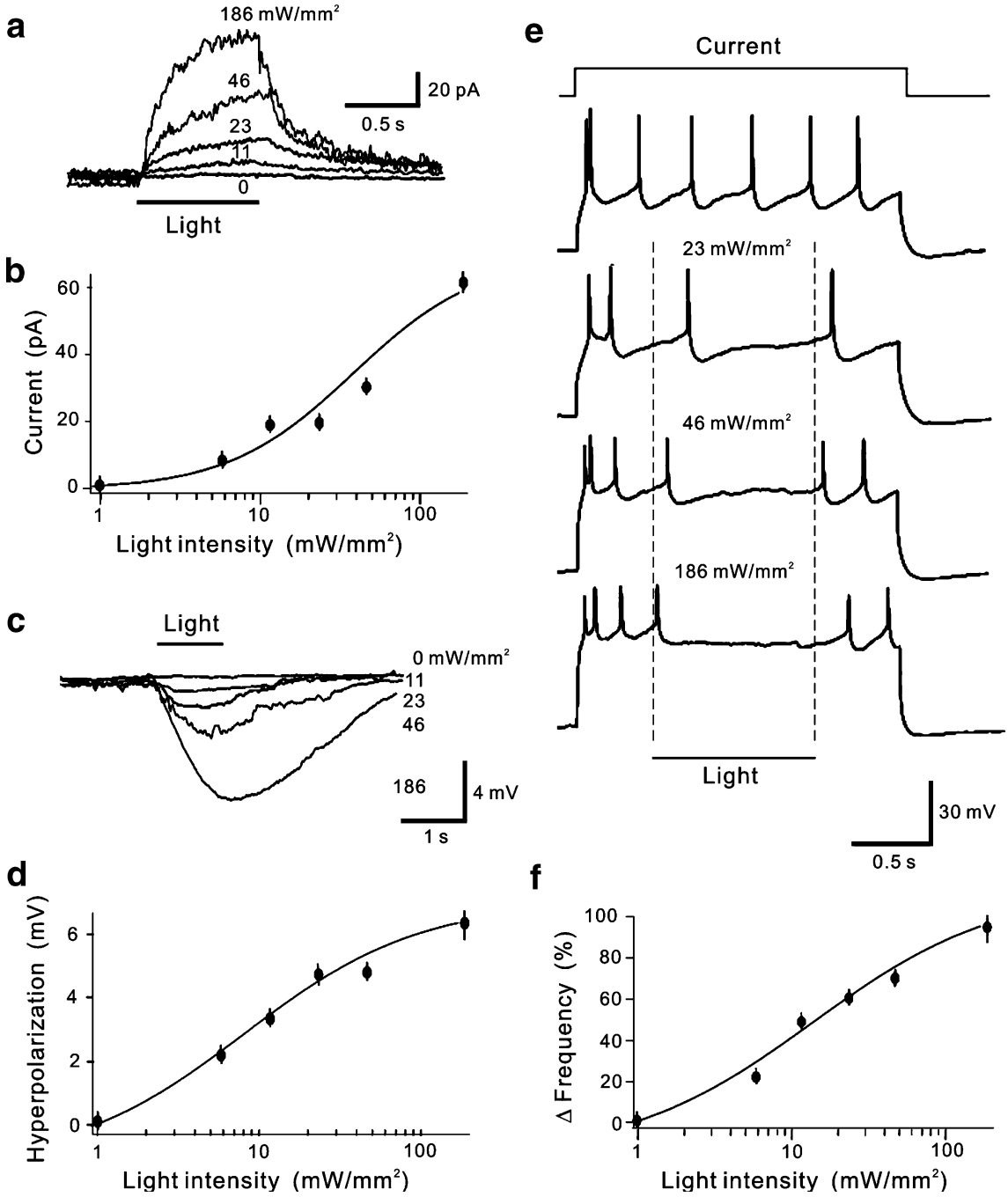

Fig. 3. Light-induced photoinhibition in NpHR-expressing neurons of Thy1-NpHR-YFP mice. (a, b) Illumination evokes photocurrents in NpHR-positive neurons ($n = 5$). (a) Light pulses of 1 s duration generated photocurrents whose amplitude depended upon light intensity. (b) Relationship between photocurrent amplitude and light intensity. Curve is fit of the Hill equation. (c, d) Light-induced hyperpolarization in NpHR-positive neurons ($n = 5$). (c) Illumination of neurons with light of variable intensity induced proportionate changes in the membrane potential of NpHR-positive neurons. (d) Relationship between light intensity and voltage changes. Curve is fit of Hill equation. (e, f) Illumination controls frequency of action potentials. (e) Light of varying luminance inhibited neuronal firing in a light intensity-dependent manner. (f) Relationship between light intensity and light-induced reduction of the AP frequency ($n = 11$). Curve is fit of the Hill equation.

$n = 11$). Fits of the Hill equation (Fig. 3f) indicated a half-maximal light intensity of 18 $\pm$ 0.1 mW/mm^2 and a Hill coefficient of 1.1 $\pm$ 0.1, again similar to the values determined in Fig. 3b and d. The maximum reduction of action potential frequency was 100% during light flashes. Together these data demonstrate that NpHR is an effective tool in silencing neuronal activity when genetically targeted and chronically expressed in transgenic mice.

Intracellular blebs represent ER retention of NpHR-YFP

Even though these physiological results demonstrate that NpHR-YFP expressed in neurons of transgenic mice is capable of mediating photoinhibition of neuronal activity, our histological images suggest that this form of NpHR-YFP is not efficiently targeted to the plasma membrane, which would reduce efficiency of photoinhibition. Furthermore, the formation of blebs raises the concern that high levels of NpHR-YFP expression may adversely affect neuronal function. To solve this problem, we began by determining the nature of the intracellular blebs formed by NpHR-YFP. We found that similar blebs were formed when NpHR-YFP was highly expressed in cultured hippocampal neurons as well as in non-neuronal cell lines, such as HEK293T cells and COS7 cells (Fig. 4a–d). Since Thy1-ChR2-YFP mice were generated with a wildtype (codons not humanized) construct, we considered the possibility that the bleb formation in Thy1-NpHR-YFP mice might be caused by a dramatic increase in expression due to codon optimization of NpHR. However, we found that wildtype NpHR-YFP also formed blebs when expressed in cultured neurons at high levels (Fig. 4e, f).

We next used various subcellular markers to determine the compartment in which NpHR-YFP accumulated. Cotransfection of NpHR-YFP and the transferrin receptor (TfR), a marker for recycling endosomes (Harding et al., 1983), did not show any colocalization of the two proteins (Fig. 5a–a″). This indicates that the NpHR-YFP was not accumulating in recycling endosomes. Antibody staining for endogenous GM130, a marker for the Golgi apparatus (Nakamura et al., 1995), also showed that NpHR-YFP blebs did not colocalize with GM130 (Fig. 5b–b″). Thus, NpHR-YFP was not accumulating in the Golgi either. In contrast, staining with an antibody for the ER marker BiP showed precise colocalization of NpHR-YFP blebs with BiP (Fig. 5c–c″). Even in cells with low levels of NpHR-YFP expression, where no blebs were present, NpHR-YFP and BiP colocalized (Fig. 5d–d″). This suggests that significant amounts of NpHR-YFP are retained in the ER even before blebs are formed, with blebs resulting from accumulation of very high levels of NpHR-YFP in the ER.

Improved ER trafficking and membrane targeting of NpHR-YFP

Several sequence features, such as signal peptide sequences, ER retention signals, and ER export signals, affect ER trafficking and expression of integral membrane proteins (Derby and Gleeson, 2007). Scanning the amino acid sequence of NpHR did not identify any known ER retention signals except for the MDEL sequence in YFP that is similar to the known ER retention signal KDEL (Derby and Gleeson, 2007). However, mutating the MDEL motif of NpHR-YFP to MDDV did not reduce the bleb formation (data not shown). We also noticed that NpHR does not contain a typical signal peptide sequence (Bendtsen et al., 2004), so we changed the signal peptide sequence of NpHR-YFP to that of ChR2 or the β2 subunit of the neuronal nicotinic acetylcholine receptor (Fig. 6a–c). Expression in cultured hippocampal neurons showed that modifying the signal peptide sequence of NpHR-YFP was insufficient to eliminate bleb formation (Fig. 6d–f).

We next determined whether addition of a conserved ER exporting sequence to NpHR-YFP would reduce bleb formation. For this purpose, we attached the ER export sequence NANSFCYENEVALTSK (Ma et al., 2001) to the carboxyl terminus of NpHR-YFP. NpHR-YFP containing the ER export signal (eNpHR-YFP) showed dramatically improved membrane targeting and diminished bleb formation in COS7 cells (Fig. 6g–i). Most importantly, expression of eNpHR-YFP in cultured hippocampal neurons did not yield blebs and showed improved plasma membrane targeting (Fig. 6j–l). Thus, by modifying the signal peptide sequence and adding an ER export signal, we generated a version of NpHR-YFP that has much-improved trafficking and should, therefore, be better for light-induced inhibition of neuronal activity.

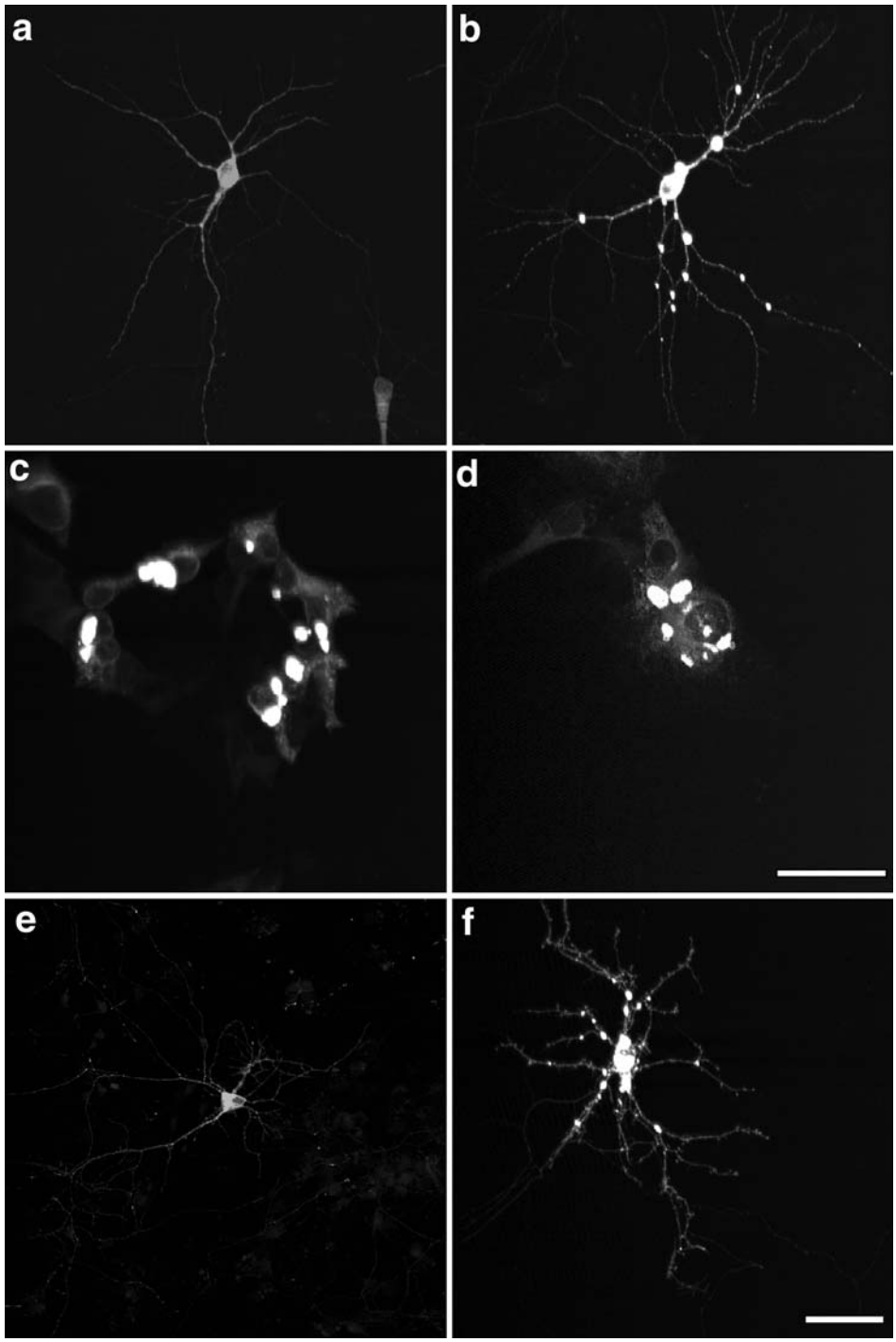

Fig. 4. High levels of NpHR-YFP expression form intracellular blebs *in vitro*. (a) NpHR-YFP expressed at low levels in cultured hippocampal neurons. (b) High levels of NpHR-YFP expression in cultured hippocampal neurons leads to the formation of numerous intracellular blebs. (c, d) Blebs also form in HEK293T cells (c) and COS7 cells (d) expressing NpHR-YFP. (e, f) Wildtype (codon not humanized) NpHR-YFP forms blebs at high levels of expression (f) but not at low levels of expression (e). Scale bar, 50 μm in d for c and d, 100 μm in f for a, b, e and f.

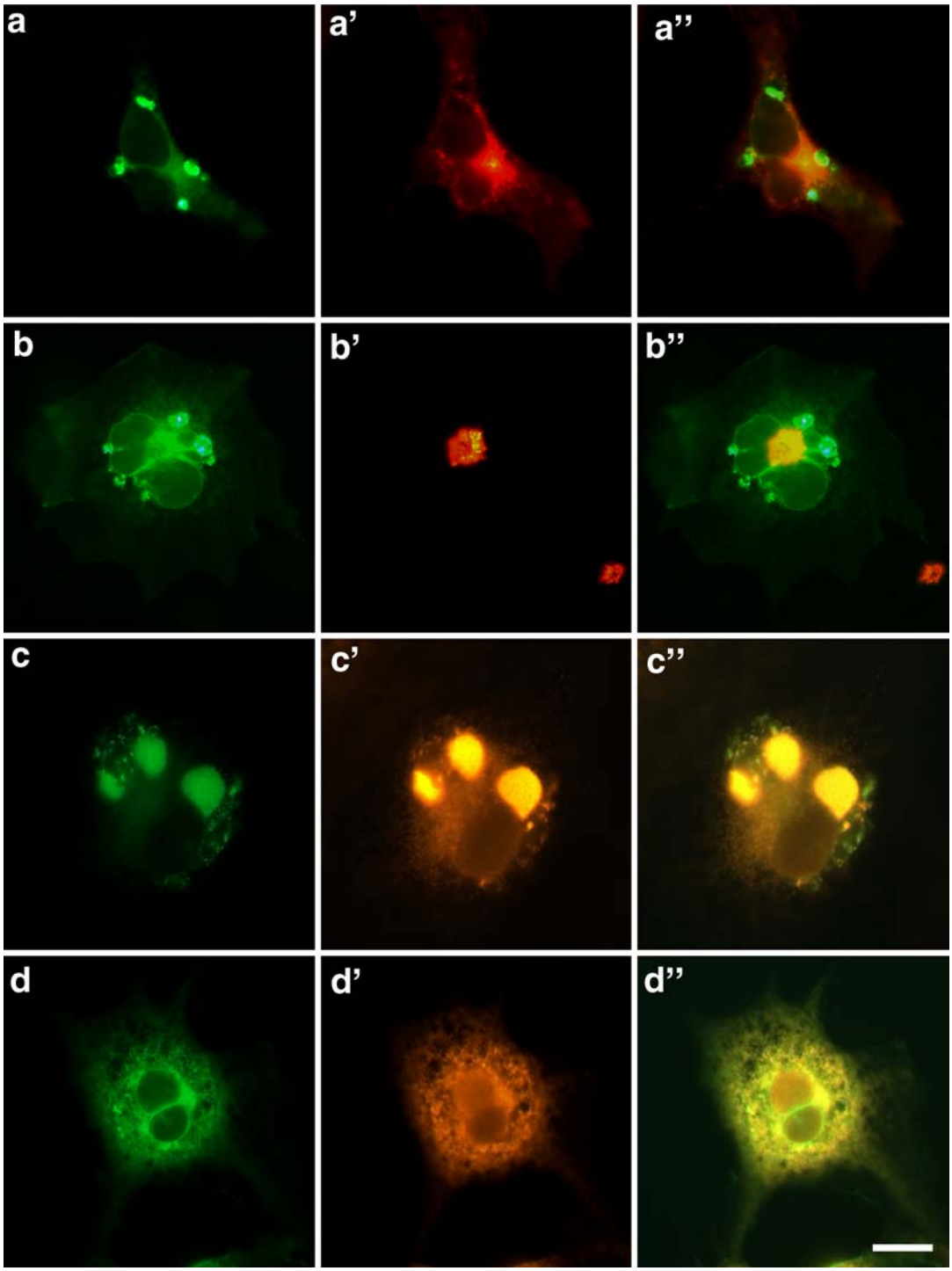

Fig. 5. The blebs correspond to retention of NpHR-YFP in the ER. (a–a′′) NpHR-YFP (a) co-expressed with transferrin receptor (TfR, red in a′) in COS7 cells. Their colocalization is not detectable (merged image in a′′). (b–b′′) COS7 cells transfected with NpHR-YFP (b) and stained with Golgi marker GM130 (b′). GM130 does not colocalize with the blebs (merged image in b′′). (c–d′′) NpHR-YFP precisely colocalizes with the ER marker BiP in COS7 cells with (c–c′′) or without (d–d′′) blebs. Scale bar, 20 μm in d′′ for a–d′′.

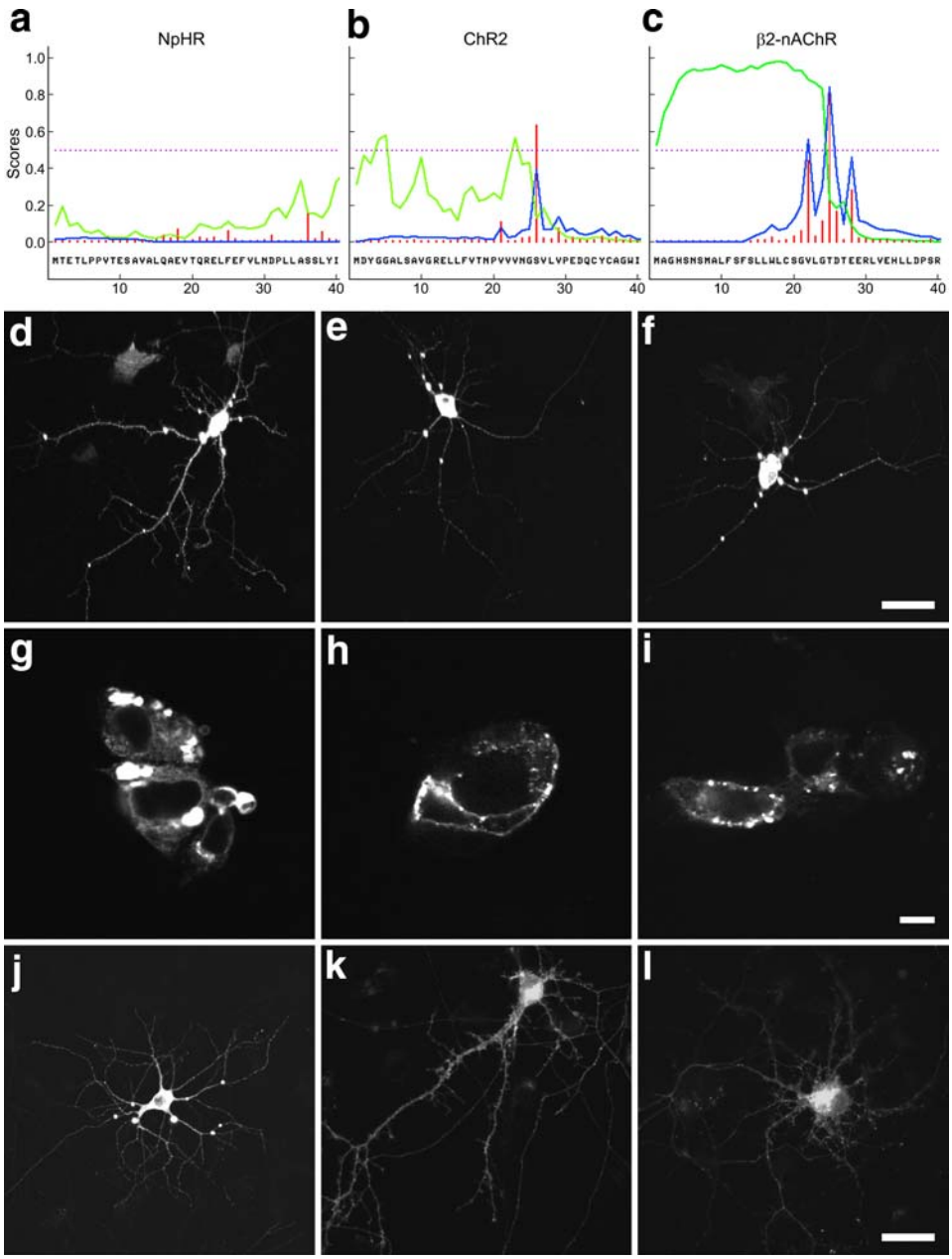

Fig. 6. Adding an ER export motif to NpHR eliminates the formation of blebs. (a) Signal peptide prediction using SignalP 3.0 software (Bendtsen et al., 2004) gives a poor score for NpHR. (b) ChR2 has a much better score for the prediction of a signal peptide than NpHR. (c) The nAChR β2 subunit has a near-perfect signal peptide sequence. Green plot indicates signal peptide prediction score (S-score); red plot indicates cleavage site prediction score (C-score); blue plot indicates the combined cleavage site prediction score from S-score and C-score (Y-score). (d–f) Improvement of signal peptide sequence alone is not sufficient to eliminate the bleb formation of NpHR-YFP in cultured hippocampal neurons; (d) NpHR-YFP with native signal peptide, (e) NpHR-YFP with ChR2 signal peptide, and (f) NpHR-YFP with the nAChR β2 subunit signal peptide. (g–i) Adding an ER export signal sequence to NpHR-YFP eliminates bleb formation in COS7 cells; (g) original NpHR-YFP without ER export signal, (h) original NpHR with ER export signal, (i) NpHR with the β2 nAChR signal peptide and ER export signal. (j–l) Adding an ER export signal sequence to NpHR-YFP eliminates bleb formation in cultured hippocampal neurons; (j) original NpHR-YFP without ER export signal, (k) original NpHR with ER export signal, (l), NpHR with the β2 nAChR signal peptide and ER exporting signal. Scale bars, 100 μm in f for d–f, 20 μm in i for g–i, 100 μm in l for j–l.

Discussion

Several chemical genetic approaches have been developed to silence neuronal activity in mammalian neurons (Tervo and Karpova, 2007). These methods allow perturbation of neuronal activity in specific subpopulations of neurons by genetic targeting and administration of chemical inducers, enabling neuroscientists to probe how individual groups of neurons regulate circuitry activity and behavior (Karpova et al., 2005; Tan et al., 2006; Armbruster et al., 2007; Lerchner et al., 2007; Wulff et al., 2007). The major advantages of these chemical genetic approaches are their on-and-off inducibility, their ability to silence large numbers of neurons and their ability to reach deep brain regions through systemic administration of chemical inducers. The major disadvantages are the slow time course of onset/offset (minutes in cultured neurons and hours to days *in vivo*) and the potential toxicity or interference with physiological processes by chemical inducers (Tervo and Karpova, 2007).

The recent development of optogenetic tools for manipulating neuronal activity with spatial and temporal precision provides an unprecedented opportunity to dissect functional circuitry connectivity and to probe the neural basis of complex behaviors (Nagel et al., 2005; Deisseroth et al., 2006; Schroll et al., 2006; Adamantidis et al., 2007; Zhang et al., 2007b; Huber et al., 2008). As a light-induced silencer, NpHR has the advantages of rapid onset/offset (in milliseconds) and spatial precision determined by the size and position of the light source. To complement the existing Thy1-ChR2-YFP transgenic mice for photoactivation of neurons (Arenkiel et al., 2007; Wang et al., 2007), in this study we generated Thy1-NpHR-YFP transgenic mice for light-induced silencing of neuronal activity. We demonstrated that illumination of NpHR-positive neurons in acute brain slices led to hyperpolarization of neurons and produced rapid, reversible inhibition of neuronal firing. Thus, in principle NpHR in transgenic mice silences neurons in a light-inducible manner, raising the potential for its targeting to genetically distinct subpopulations of neurons in order to determine how neuronal activity in each neuron subtype shapes circuitry function and behavior.

Despite this great promise, we found that the current form of NpHR has two major problems when expressed in transgenic mice: poor membrane targeting and bleb formation due to ER retention. The poor expression on the plasma membrane could lower the efficiency of light-induced inhibition of neuronal activity. In cultured hippocampal neurons transfected with NpHR-YFP, the light intensity required to achieve near 100% inhibition of neuronal firing is 21.7 mW/mm^2 at the sample in cultured neurons (Zhang et al., 2007a). While it is difficult to directly compare these measurements to the slice experiments described here, it is likely that lower membrane expression in Thy1-NpHR-YFP line 6 mice contributed to our observation that higher light intensities (≥186 mW/mm^2) were required for 100% inhibition of cortical pyramidal cells. However, higher levels of expression in transgenic mice lead to the formation of numerous intracellular blebs, discouraging us from using these mice for further experiments. In addition, we found that if NpHR is highly expressed in cultured neurons or even in non-neuronal cell lines it forms similar blebs as observed in neurons of the transgenic mice, suggesting a general defect in trafficking of NpHR to the plasma membrane. Although the mechanism of ER retention is unclear—we did not find any known ER retention signals in the NpHR sequence—our modification, through replacement of the signal peptide and the addition of an ER export signal, has resulted in a much improved version of NpHR-YFP for light-induced silencing of neuronal activity. A similarly modified eNpHR has also been shown to have increased peak photocurrent compared to the original NpHR (Gradinaru et al., 2008). Thus, future transgenic mice expressing the improved eNpHR in neurons will likely be a valuable tool for probing circuitry function.

Methods

All animal procedures listed here were approved by the Duke University Institutional Animal Care and Use Committee.

Generation of Thy1-NpHR transgenic mice

Humanized NpHR from pcDNA3.1/NpHR-EYFP (Zhang et al., 2007a) was cut out with NheI and XbaI digestion, blunted, and subcloned into the mouse Thy1 vector (Caroni, 1997; Feng et al.,

2000). Transgenic mice were generated by the injection of the gel purified Thy1-NpHR-YFP DNA construct into fertilized oocytes, using standard pronuclear injection techniques (Feng et al., 2004). Fertilized eggs were collected from the matings between C57BL/6J and CBA F1 hybrids. Transgenic founders were identified through tail DNA PCR using primers for Thy1 and NpHR (Thy1F1, TCTGAGTGGCAAAGGACCTTAGG; NpHRR1, TCCACCAGCAGGATATACAAGACC), which amplify a 750 bp fragment. The transgenic lines generated were backcrossed to C57BL/6. Of 7 founder lines established, 5 showed NpHR-YFP expression.

Anatomy

To assess the expression of NpHR-YFP, mice were anesthetized with an overdose of isoflurane and perfused transcardially with 0.1 M phosphate buffered saline (PBS) followed by 4% paraformaldehyde in PBS. Brains were cut into 50 μm thick slices on a vibratome. Fluorescence images (4$\times$ objective) were obtained with an AxioImager microscope (Zeiss) and Axiocam *HRc* camera or a Nikon confocal microscope (20$\times$ objective). Image montages were assembled with Photoshop Elements software.

Brain slice recording and photoinhibition

For recordings of neuronal electrophysiological properties, 250–350 μm thick slices were prepared from the cortex and hippocampus of 13- to 36-day-old line 6 mice using procedures were approved by the Animal Care and Use Committee of Duke University. Whole-cell patch clamp recordings were made with an Axoclamp 2B amplifier (Axon Instruments, Foster City, CA), acquired with Clampfit (Axon Instruments), and analyzed with Igor Pro. Recording pipettes had resistances of 2–7 MΩ and contained 130 mM K-gluconate, 2 mM NaCl, 4 mM $MgCl_2$, 20 mM Hepes, 4 mM Na_2ATP, 0.4 mM NaGTP, and 250 μM K-EGTA (pH 7.3). The extracellular solution consisted of 125 mM NaCl, 2.5 mM KCl, 2 mM $CaCl_2$, 1 or 1.3 mM $MgCl_2$, 20 mM dextrose or D-glucose, 1.25 mM NaH_2PO4, and 26 mM $NaHCO_3$, (pH 7.4 after bubbling with 95% O_2/5% CO_2). A junction potential of 10 mV was taken into account when reporting membrane potentials. Experiments were performed at room temperature (21–24°C). Slices were examined on an upright epifluorescence microscope (Eclipse E600-FN; Nikon). For identifying NpHR-expressing neurons, the fluorescence of YFP fused to NpHR (515–555 nm) was detected with a CoolSNAP-fx camera (Photometrics, Tucson, AZ). For activating NpHR, the same arc lamp was used to create bandpass-filtered light pulses (545–585 nm), with light pulse duration controlled by an electronic shutter (Uniblitz; Vincent Associates, Rochester, NY).

Constructs

Information for pcDNA3.1/wildtype NpHR-YFP and pcDNA3.1/NpHR-EYFP can be obtained from the Karl Deisseroth lab website at Stanford University (http://www.stanford.edu/group/dlab/optogenetics/sequence_info.html). pCMV-ChR2SP-NpHR-YFP was produced by the replacement of the first 27 amino acids of NpHR with the signal peptide of hChR2 (MDYGGALSAVGRELLFVTNPVVVNGS). pCMV-β2SP-NpHR-YFP was prepared by the replacement of the NpHR signal peptide with the β2 subunit signal peptide of the neuronal nicotinic acetylcholine receptor (MAGHSNSMALFSFSLLW LCSGVLGTEF). pCMV/eNpHR-YFP, pCMV/ChR2SP-eNpHR-YFP, and pCMV/β2SP-eNpHR-YFP were prepared by fusing the 16 amino acids from 373 to 385 of the potassium channel Kir2.1 (NANSFCYENEVALTSK) to the C-terminus of NpHR-YFP.

Antibodies

Mouse anti-GM130 monoclonal antibody (ab1299, 1:500 dilutions) and Rabbit anti-GRP78 BiP (ab21685, 1:200 dilutions) were from Abcam.

Cell culture and transfection

293T cells were cultured in DMEM/F12 supplemented with 10% FBS and 1% penicillin/streptomycin. COS7 cells were cultured in DMEM with 10% FBS, non-essential amino acids and 1% penicillin/streptomycin. Hippocampal neuron cultures were prepared from E18 rat embryos as described (Ehlers, 2000). Cells were transfected with Lipofectamine 2000 (Invitrogen) according to the manufacturer's recommendations.

Acknowledgments

We thank João Peça and Mary (Molly) Heyer for their help in the preparation of this manuscript. We

thank members of the Feng lab for their support. We also thank members of the lab of Michael Ehlers for technical help. This work was supported by NIH grants to K. Deisseroth, G. J. Augustine, and G. Feng.

References

Adamantidis, A. R., Zhang, F., Aravanis, A. M., Deisseroth, K., and de Lecea, L. (2007). Neural substrates of awakening probed with optogenetic control of hypocretin neurons. Nature *450*, 420–424.

Arenkiel, B. R., Peca, J., Davison, I. G., Feliciano, C., Deisseroth, K., Augustine, G. J., Ehlers, M. D., and Feng, G. (2007). *In vivo* light-induced activation of neural circuitry in transgenic mice expressing channelrhodopsin-2. Neuron *54*, 205–218.

Armbruster, B. N., Li, X., Pausch, M. H., Herlitze, S., and Roth, B. L. (2007). Evolving the lock to fit the key to create a family of G protein-coupled receptors potently activated by an inert ligand. Proc. Natl. Acad. Sci. USA *104*, 5163–5168.

Bendtsen, J. D., Nielsen, H., von Heijne, G., and Brunak, S. (2004). Improved prediction of signal peptides: SignalP 3.0. J. Mol. Biol. *340*, 783–795.

Bi, A., Cui, J., Ma, Y. P., Olshevskaya, E., Pu, M., Dizhoor, A. M., and Pan, Z. H. (2006). Ectopic expression of a microbial-type rhodopsin restores visual responses in mice with photoreceptor degeneration. Neuron *50*, 23–33.

Boyden, E. S., Zhang, F., Bamberg, E., Nagel, G., and Deisseroth, K. (2005). Millisecond-timescale, genetically targeted optical control of neural activity. Nat. Neurosci. *8*, 1263–1268.

Caroni, P. (1997). Overexpression of growth-associated proteins in the neurons of adult transgenic mice. J. Neurosci. Methods *71*, 3–9.

Deisseroth, K., Feng, G., Majewska, A., Ting, A. E., Miesenböck, G., and Schnitzer, M. J. (2006). Next-generation optical technologies for illuminating genetically-targeted brain circuits. J. Neurosci. *26*, 10380–10386.

Derby, M. C. and Gleeson, P. A. (2007). New insights into membrane trafficking and protein sorting. Int. Rev. Cytol. *261*, 47–116.

Ehlers, M. D. (2000). Reinsertion or degradation of AMPA receptors determined by activity-dependent endocytic sorting. Neuron *28*, 511–525.

Ernst, O. P., Sánchez Murcia, P. A., Daldrop, P., Tsunoda, S. P., Kateriya, S., and Hegemann, P. (2008). Photoactivation of channelrhodopsin. J. Biol. Chem. *283*, 1637–1643.

Feng, G., Hood, R., Bernstein, M., Keller-Peck, C., Nguyen, Q., Wallace, M., Nerbonne, J. M., Litchman, J. W., and Sanes, J. R. (2000). Imaging neuronal subsets in transgenic mice expressing multiple spectral variants of GFP. Neuron *28*, 41–51.

Feng, G., Lu, J., and Gross, J. (2004). Generation of transgenic mice. Methods Mol. Med. *99*, 255–267.

Gradinaru, V., Thompson, K. R., and Deisseroth, K. (2008). eNpHR: a Natronomonas halorhodopsin enhanced for optogenetic applications. Brain Cell Biol. 2008 Aug 2 [Epub ahead of print].

Gradinaru, V., Thompson, K. R., Zhang, F., Mogri, M., Kay, K., Schneider, M. B., and Deisseroth, K. (2007). Targeting and readout strategies for fast optical neural control *in vitro* and *in vivo*. J. Neurosci. *27*, 14231–14238.

Han, X. and Boyden, E. S. (2007). Multiple-color optical activation, silencing, and desynchronization of neural activity, with single-spike temporal resolution. PLoS ONE *2*, e299.

Harding, C., Heuser, J., and Stahl, P. (1983). Receptor-mediated endocytosis of transferrin and recycling of the transferring receptor in rat reticulocytes. J. Cell Biol. *97*, 329–339.

Huber, D., Petreanu, L., Ghitani, N., Ranade, S., Hromádka, T., Mainen, Z., and Svoboda, K. (2008). Sparse optical microstimulation in barrel cortex drives learned behaviour in freely moving mice. Nature *451*, 61–64.

Karpova, A. Y., Tervo, D. G., Gray, N. W., and Svoboda, K. (2005). Rapid and reversible chemical inactivation of synaptic transmission in genetically targeted neurons. Neuron *48*, 727–735.

Kolbe, M., Besir, H., Essen, L. O., and Oesterhelt, D. (2000). Structure of the light-driven chloride pump halorhodopsin at 1.8 A resolution. Science *288*, 1390–1396.

Lanyi, J. K. (1990). Halorhodopsin, a light-driven electrogenic chloride-transport system. Physiol. Rev. *70*, 319–330.

Lanyi, J. K., Duschl, A., Hatfield, G. W., May, K., and Oesterhelt, D. (1990). The primary structure of a halorhodopsin from *Natronobacterium pharaonis*. Structural, functional and evolutionary implications for bacterial rhodopsins and halorhodopsins. J. Biol. Chem. *265*, 1253–1260.

Lerchner, W., Xiao, C., Nashmi, R., Slimko, E. M., van Trigt, L., Lester, H. A., and Anderson, D. J. (2007). Reversible silencing of neuronal excitability in behaving mice by a genetically targeted, ivermectingated Cl^- channel. Neuron *54*, 35–49.

Li, X., Gutierrez, D. V., Hanson, M. G., Han, J., Mark, M. D., Chiel, H., Hegemann, P., Landmesser, L. T., and Herlitze, S. (2005). Fast noninvasive activation and inhibition of neural and network activity by vertebrate rhodopsin and green algae channelrhodopsin. Proc. Natl. Acad. Sci. USA *102*, 17816–17821.

Ma, D., Zerangue, N., Lin, Y. F., Collins, A., Yu, M., Jan, Y. N., and Jan, L. Y. (2001). Role of ER export signals in controlling surface potassium channel numbers. Science *291*, 316–319.

Nagel, G., Brauner, M., Liewald, J. F., Adeishvili, N., Bamberg, E., and Gottschalk, A. (2005). Light activation of channelrhodopsin-2 in excitable cells of *Caenorhabditis elegans* triggers rapid behavioral responses. Curr. Biol. *15*, 2279–2284.

Nagel, G., Szellas, T., Huhn, W., Kateriya, S., Adeishvili, N., Berthold, P., Ollig, D., Hegemann, P., and Bamberg, E. (2003). Channelrhodopsin-2, a directly light-gated cation-selective membrane channel. Proc. Natl. Acad. Sci. USA *100*, 13940–13945.

Nakamura, N., Rabouille, C., Watson, R., Nilsson, T., Hui, N., Slusarewicz, P., Kreis, T. E., and Warren, G. (1995). Characterization of a cis-Golgi matrix protein, GM130. J. Cell Biol. *131*, 1715–1726.

Petreanu, L., Huber, D., Sobczyk, A., and Svoboda, K. (2007). Channelrhodopsin-2-assisted circuit mapping of long-range callosal projections. Nat. Neurosci. *10*, 663–668.

Schroll, C., Riemensperger, T., Bucher, D., Ehmer, J., Völler, T., Erbguth, K., Gerber, B., Hendel, T., Nagel, G., Buchner, E., and Fiala, A. (2006). Light-induced activation of distinct modulatory neurons triggers appetitive or aversive learning in Drosophila larvae. Curr. Biol. *16*, 1741–1747.

Tan, E. M., Yamaguchi, Y., Horwitz, G. D., Gosgnach, S., Lein, E. S., Goulding, M., Albright, T. D., and Callaway, E. M. (2006). Selective and quickly reversible inactivation of mammalian neurons *in vivo* using the Drosophila allatostatin receptor. Neuron *51*, 157–170.

Tervo, D. and Karpova, A. Y. (2007). Rapidly inducible, genetically targeted inactivation of neural and synaptic activity *in vivo*. Curr. Opin. Neurobiol. *17*, 581–586.

Wang, H., Peca, J., Matsuzaki, M., Matsuzaki, K., Noguchi, J., Qiu, L., Wang, D., Zhang, F., Boyden, E., Deisseroth, K., Kasai, H., Hall, W. C., Feng, G., and Augustine, G. J. (2007). High-speed mapping of synaptic connectivity using photostimulation in Channelrhodopsin-2 transgenic mice. Proc. Natl. Acad. Sci. USA *104*, 8143–8148.

Wulff, P., Goetz, T., Leppä, E., Linden, A. M., Renzi, M., Swinny, J. D., Vekovischeva, O. Y., Sieghart, W., Somogyi, P., Korpi, E. R., Farrant, M., and Wisden, W. (2007). From synapse to behavior: rapid modulation of defined neuronal types with engineered GABAA receptors. Nat. Neurosci. *10*, 923–929.

Zhang, F., Aravanis, A. M., Adamantidis, A., de Lecea, L., and Deisseroth, K. (2007). Circuit-breakers: optical technologies for probing neural signals and systems. Nat. Rev. Neurosci. *8*, 577–581.

Zhang, Y. P. and Oertner, T. G. (2007). Optical induction of synaptic plasticity using a light-sensitive channel. Nat. Methods *4*, 139–141.

Zhang, F., Prigge, M., Beyrière, F., Tsunoda, S. P., Mattis, J., Yizhar, O., Hegemann, P., and Deisseroth, K. (2008). Red-shifted optogenetic excitation: a tool for fast neural control derived from *Volvox carteri*. Nat. Neurosci. *11*, 631–633.

Zhang, F., Wang, L. P., Boyden, E. S., and Deisseroth, K. (2006). Channelrhodopsin-2 and optical control of excitable cells. Nat. Methods *3*, 785–792.

Zhang, F., Wang, L. P., Brauner, M., Liewald, J. F., Kay, K., Watzke, N., Wood, P. G., Bamberg, E., Nagel, G., Gottschalk, A., and Deisseroth, K. (2007). Multimodal fast optical interrogation of neural circuitry. Nature *446*, 633–639.